

Microstructural Characteristics and Mechanical Properties of Low-Alloy, Medium-Carbon Steels After Multiple Tempering

LUO, Quanshun <<http://orcid.org/0000-0003-4102-2129>>, ABBASI, Erfan <<http://orcid.org/0000-0001-6252-5425>> and OWENS, Dave

Available from Sheffield Hallam University Research Archive (SHURA) at:

<https://shura.shu.ac.uk/22499/>

This document is the Accepted Version [AM]

Citation:

LUO, Quanshun, ABBASI, Erfan and OWENS, Dave (2018). Microstructural Characteristics and Mechanical Properties of Low-Alloy, Medium-Carbon Steels After Multiple Tempering. *Acta Metallurgica Sinica*, 32 (1), 74-88. [Article]

Copyright and re-use policy

See <http://shura.shu.ac.uk/information.html>

Highlights

1. Hardness reduction after tempering is primarily controlled by tempering temperature.
2. NiCrMoV steel showed a higher temper resistant compared to NiCrSi steel.
3. Retained austenite decomposition is mainly dependent upon the tempering temperature.
4. Precipitation along lath martensite boundaries enhances tempered martensite embrittlement.
5. The formation of precipitates during tempering can considerably control the toughness of steel.

Microstructural Characteristics and Mechanical Properties of Low Alloy Wear Resistant Steels after Multiple Tempering

Erfan Abbasi ^{a,b,*}, Quanshun Luo ^a, Dave Owens ^b

^a Materials and Engineering Research Institute, Sheffield Hallam University, Howard Street, Sheffield, S1 1WB, UK

^b Tyzack Machine Knives Ltd, Shepcote Lane, Sheffield, S9 1TG, UK

* Corresponding author. Tel.: +44 (0) 114 221 1059

E-mail address: engabasi@gmail.com (E. Abbasi)

The microstructure and mechanical properties of NiCrMoV- and NiCrSi-alloyed medium-carbon steels were investigated after multiple tempering. After austenitising, the steels were hardened by oil quenching and subsequently double or triple tempered at temperatures from 250 to 500 °C. The samples were characterised using scanning electron microscopy and X-ray diffraction, while the mechanical properties were evaluated by Vickers hardness testing, V-notched Charpy impact testing and tensile testing. The results showed that the retained austenite was stable up to 400 °C and the applied multiple tempering below this temperature did not lead to a complete decomposition of retained austenite in both steels. It was also found that the microstructure, hardness and impact toughness varied mainly as a function of tempering temperature, regardless of the number of tempering stages. Moreover, the impact toughness of NiCrMoV steel was rather similar after single/triple tempering at different temperatures, while NiCrSi steel exhibited tempered martensite embrittlement after single/double tempering at 400 °C. The observed difference was mainly attributed to the effect of precipitation behaviour due to the effect of alloying additions in the studied steels.

Keywords: Medium-carbon steels; Multiple tempering; Alloying addition; Mechanical properties; Retained austenite

1. Introduction

In wear-resistant components, a combination of toughness, hardness and strength is normally required to improve their wear performance [1, 2]. In this context, medium-carbon steels with a tensile strength of over 1000 MPa are extensively used in automotive, military and tool-making industries, especially for wear resistance under severe loading conditions [3, 4]. However, a required superior wear performance, especially under more severe working environments, has driven the need for modifications in the alloy design and manufacturability

of these steels. The wear-resistant steel components are widely produced through quenching and tempering [5]. In this case, many investigations have been reported on the effect of multiple tempering on the microstructure and mechanical properties of alloyed steels [6–9]. It is well known that during single/multiple tempering and at different tempering temperatures, various transformations occur which mainly consisted of Fe/alloy carbides precipitation, recovery of martensite, decomposition of retained austenite, growth/coarsening/spheroidisation of Fe/alloy carbides and the segregation of alloying elements and impurities [10, 11]. Furthermore, double or multiple tempering is conventionally used for different steels in terms of their chemical composition and final application to further decompose retained austenite, to enhance toughness and to reduce quenching defects.

In recent years, efforts have been made to employ small additions of alloying elements, especially microalloy elements, to increase tempering resistance, to control the microstructure and to reduce hydrogen embrittlement susceptibility during tempering [5, 12–14]. However, no comparative study has focused on the effects of small additions of alloying elements in low-alloy, medium-carbon steels on the microstructural evolution and its relationship with mechanical properties during each stage of multiple tempering. This can further clarify the effects of small alloying additions on microstructure which can be used as an approach in controlling the mechanical properties, wear resistance and processing defects [15]. Therefore, a systematic study was performed on two low-alloy, medium-carbon, wear-resistant steels (namely, NiCrSi and NiCrMoV steels) during double or triple tempering to better understand the effect of chemical composition on their microstructure and mechanical properties, especially hardness and toughness, at each tempering stage and different tempering temperatures.

2. Experimental Procedure

The materials used in this investigation included two hot rolled steels with different alloying contents (Table 1). The studied steels are hereafter referred to as “NiCrSi” and “NiCrMoV” steels. The NiCrMoV steel was produced through vacuum induction melting and electroslag remelting (VIM-ESR), and NiCrSi steel was cast by electric arc melting, ladle arc melting and vacuum degassing. These steels are designed to produce shear blades to perform under severe impact/sliding wear conditions. The NiCrSi and NiCrMoV steels are received in fully annealed conditions, and they are normally tempered after oil quenching to minimise the risk of quenching defects and improve their wear performance under service conditions.

The quenching-tempering heat treatments were carried out using samples with a size of 40×60×100 mm³. During quench-hardening, NiCrSi and NiCrMoV samples were held for 1.5 h and directly immersed-agitated in oil from 850 and 900 °C, respectively. Samples were cooled to about 100 °C in oil with an average cooling rate of about 4 °C/s in order to minimise any possible quenching defects and were immediately transferred in a preheated tempering furnace [15,16]. The volume fraction of martensite was estimated using the following equation [17].

Table 1, Chemical composition of investigated steels (wt%).

Steel	C	Si	Mn	Cr	V	Mo	Ni	Ti	B	S	P	Fe
NiCrSi	0.36	0.89	0.60	0.9	-	0.06	3.11	-	-	0.010	-	Bal.
NiCrMoV	0.50	0.22	0.65	1.33	0.52	0.77	3.70	0.002	-	-	-	Bal.

$$\text{Vol}_{\text{martensite}}=1-\exp(-\alpha_m(T_{\text{th}}-T_Q)) \quad (1)$$

where T_{th} is the theoretical martensite start temperature and T_Q is the quenching temperature. α_m is the chemical composition rate parameter and is calculated using a simple linear equation, as below.

$$\alpha_m=0.0224-0.0107x_C-0.0007x_{\text{Mn}}-0.00005x_{\text{Ni}}-0.00012x_{\text{Cr}}-0.0001x_{\text{Mo}} \quad (2)$$

The theoretical martensite start temperature of the studied steels was approximated using the following equation [18]:

$$\begin{aligned} T_{\text{th}} = & 545 - 601:2 (1 - \exp(-0.868C\%)) - 34.4\text{Mn}\% - 3.\text{Si}\% - 9.2\text{Cr}\% \\ & - 17.3\text{Ni}\% - 15.4\text{Mo}\% + 10.8\text{V}\% + 4.7\text{Co}\% - 1.4\text{Al}\% - 16.3\text{Cu}\% \\ & - 361\text{Nb}\% - 2.44\text{Ti}\% - 3448\text{B}\% \end{aligned} \quad (3)$$

The T_{th} of NiCrSi and NiCrMoV steels was determined as 302 and 254 °C, respectively. However, the initial assessment showed that about 97 and 91 (vol%) of austenite would have transformed into martensite at initial quenching temperature (i.e. 100 °C) in NiCrSi and NiCrMoV steels, respectively.

Double/triple tempering was carried out at identical holding times (2 h at each stage) and temperatures (i.e. 250, 300, 400 and 500 °C). The NiCrSi steel was double tempered and NiCrMoV steel was subjected to triple tempering, as prior experimental results have shown that these conditions provide a proper wear resistant in service [19]. Note that the lifetime of triple-tempered NiCrMoV blades is roughly two times longer than double-tempered NiCrSi blades under similar working conditions. However, the effect of tempering on the microstructure and mechanical properties was studied using separate samples after each

tempering stage. Sample preparation for microstructural characterisations was carried out according to standard procedures on both rolling and normal direction planes. Microstructural characterisations after each tempering stage were performed by Scanning Electron Microscopy (SEM) using a FEG-Nova NanoSEM at 20 kV.

The crystalline characteristics of the studied steels were studied using a PANalytical Empyrean X-ray diffractometer with Co K α radiation (i.e. including Co k α_1 ($\lambda=0.178900\text{nm}$) and Co k α_2 ($\lambda=0.179284\text{ nm}$) radiations). The retained austenite was characterised by Rietveld refinement method using the Topas Academic package software V5.0. The instrumental effects on XRD patterns were subtracted using a diffraction pattern of standard silicon sample (SRM 640e). The dislocation density of steels was approximated according to Williamson–Hall (WH) method using XRD data according to the following equation:

$$\text{Dislocation density} = 14.4 (\epsilon^2 / b^2) \quad (4)$$

where ϵ and b are microstrain and Burger's vector (0.248 nm for ferrite), respectively. The microstrain was estimated using the following equation, using all diffraction peaks.

$$\delta (\cos \theta / \lambda) = a + 2\epsilon (\sin \theta / \lambda) \quad (5)$$

$$a = 0.9 / D \quad (6)$$

where δ , θ (radians), λ , a , ϵ and D are the physical broadening of XRD peak width (i.e. Full Width Half Maximum (FWHM)), diffraction angle, X-ray wavelength and average particle size, respectively.

The hardness of studied steels was determined by Vickers hardness testing with 30 kg load and 15 s holding time before unloading. The average hardness value was calculated from ten measurements for each sample. A better comparison between the results was performed by converting HV hardness to HRC.

The mechanical properties of double-tempered NiCrSi steel and triple-tempered NiCrMoV steel were determined according to ISO-6892 using a Zwick-Roell testing machine. The elongation during the test in cylindrical dog-bone shaped tensile specimens (rolling direction) with a gauge length of 25 mm and gauge diameter of 5 mm was recorded by a non-contact high resolution laserXtens extensometer. The repeatability of results was examined using three separate samples from each steel.

The V-notched Charpy impact toughness of steels after each tempering stage was determined by V-notched Charpy impact testing using a pendulum Avery-Denison Charpy testing machine with a nominal energy of 300 J. Standard Charpy impact specimens with a size of $55 \times 10 \times 10\text{ mm}^3$ and a notch radius of 0.25 mm were tested according to ASTM E23 at room temperature. The V-notch edge and front edge of Charpy specimens were parallel to

transverse and normal directions, respectively. The repeatability of results was tested using three separate samples. The fractured Charpy impact and tensile samples were examined by SEM.

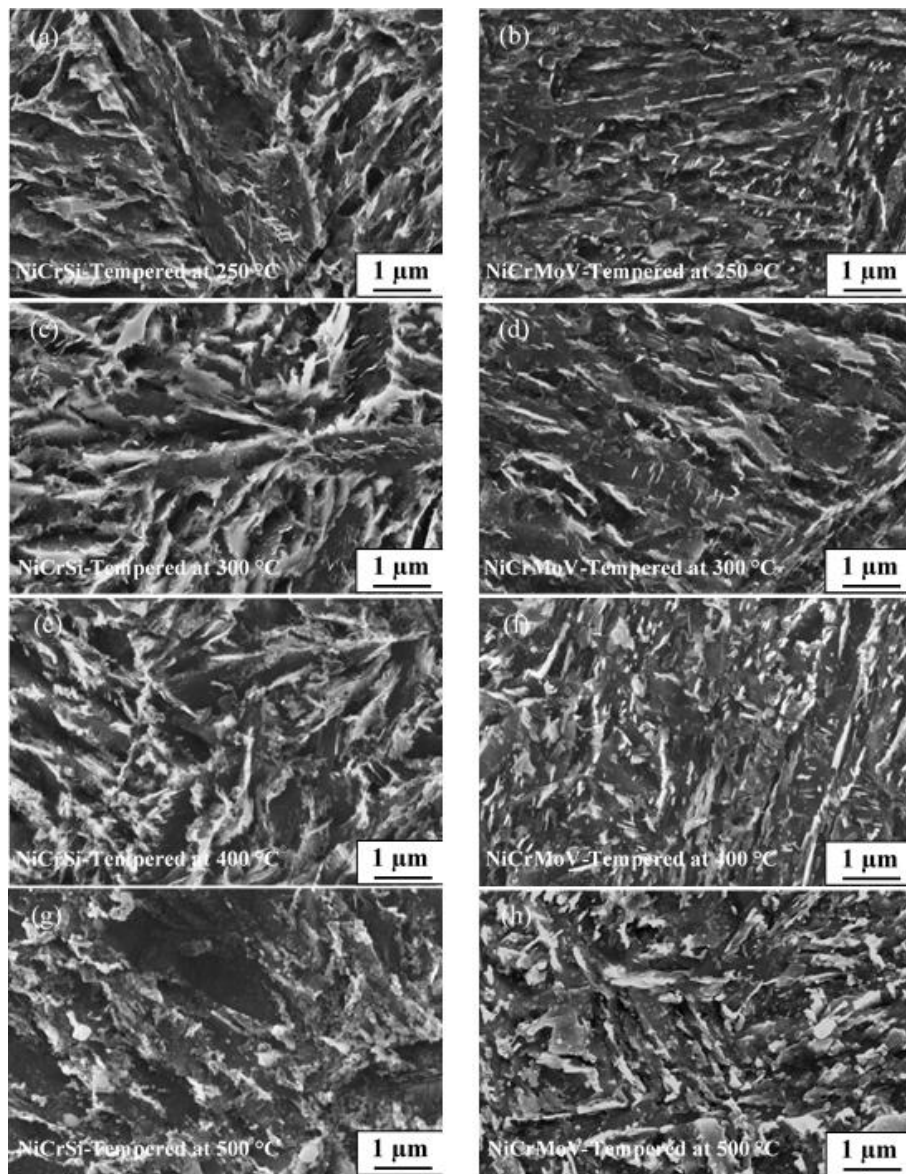


Fig. 1 SEM micrographs, corresponding to single tempered NiCrSi and NiCrMoV steels at different tempering temperatures.

3. Results

3.1. Microstructure

Figure 1 and 2 show SEM micrographs corresponding to the NiCrSi and NiCrMoV steels after single tempering at different temperatures. Microscopy observations showed a fully tempered martensite structure throughout both rolling and normal direction planes of the studied steels. From SEM analysis, it was found that the size and morphology of tempered

martensite did not change during single, double or triple tempering in both steels. After
t e m p e r i n g t h e

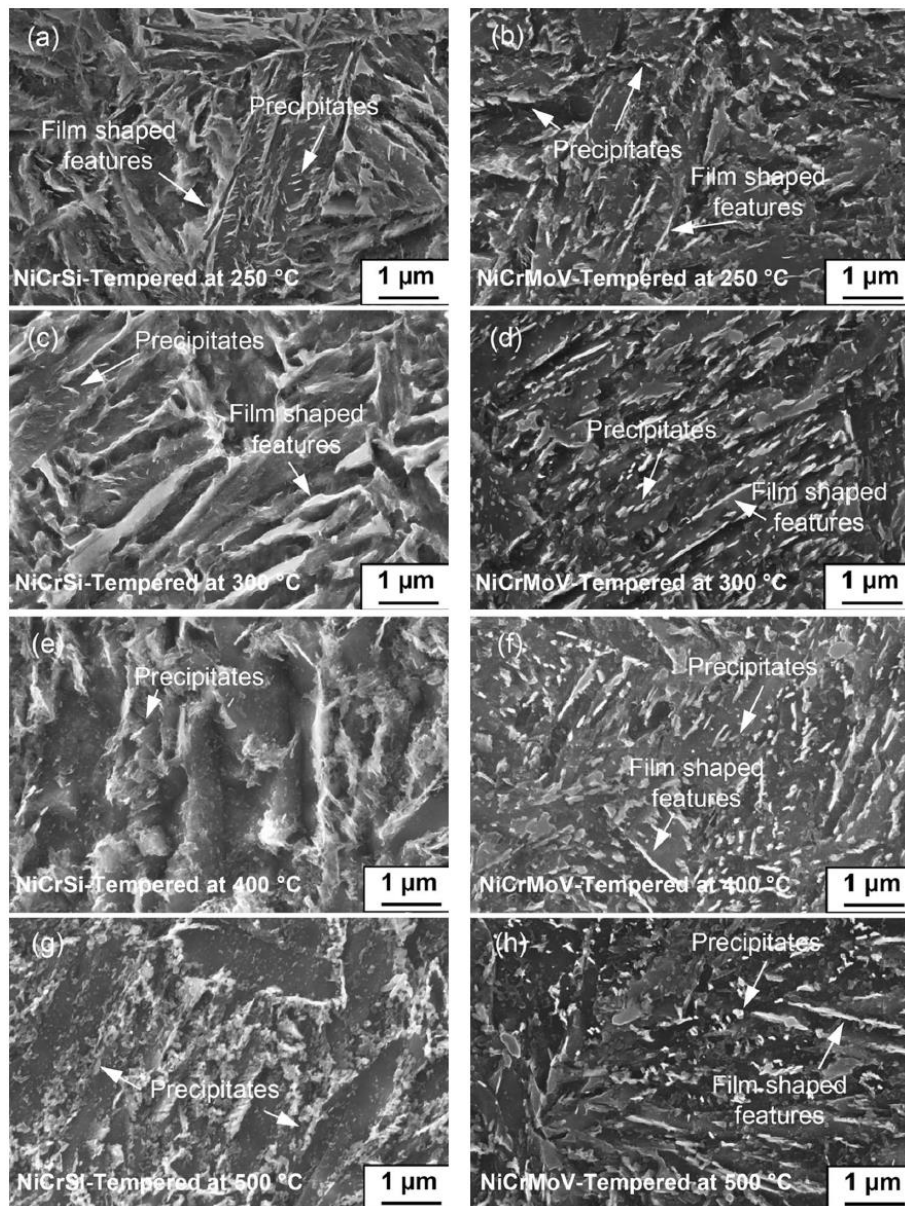


Fig. 2 Selected SEM micrographs, corresponding to double-tempered NiCrSi and triple-tempered NiCrMoV steels

microstructure of studied steels showed significant different features in the tempered martensitic structure.

In NiCrSi steel, bright filmy and blocky shaped features mainly appeared on the lath boundaries. It is thought that these bright features are related to retained austenite. By increasing the tempering temperature up to 400 °C, a large amount of nano-scale rod shaped carbide precipitates appeared in the microstructure of NiCrSi steel. Tempering at 400 - 500

°C considerably reduced the number of bright film shaped features at the expense of formation of rod and spherical shaped carbide precipitates. However, tempering at 500 °C did not show any coarsening (Ostwald ripening) of precipitates in NiCrSi steel. Moreover, the microscopy results showed insignificant variations in NiCrSi steel due to double tempering. SEM observations of NiCrMoV steel showed a large number of rod shaped interlath carbide precipitates in the microstructure after tempering at 250 °C, Figs, 1, 2. This is similar to the results of other researchers who also reported Fe₃C precipitation in AISI 4340 steel after tempering at 250 °C [21, 22]. The microstructure did not indicate any significant difference in the morphology and density of precipitates due to tempering at higher tempering temperatures (i.e. up to 400 °C) and after double/triple tempering. However, after tempering at 500 °C a larger frequency of spherical precipitates appeared in the microstructure of NiCrMoV, suggesting a possible spheroidisation phenomenon. The results suggested that a tempering at 500 °C provided conditions for the spheroidisation of precipitates, while double or triple tempering did not influence the density, size and morphology of precipitates. This is in line with the results of double tempered NiCrSi steels at all tempering temperatures, suggesting no considerable change in the growth-coarsening of precipitates due to double or triple tempering in both steels.

3.2. Retained Austenite

Figure 3a shows a selected XRD spectrum of a quenched–tempered sample. The XRD analysis revealed the presence of retained austenite and martensite in the quenched–tempered microstructure of both steels. Table 2 presents the characteristics of retained austenite, measured from XRD results. The lattice parameter of retained austenite was calculated from the extrapolation method of Nelson and Riley. Subsequently, the carbon content of retained austenite was determined from its lattice parameter (nm) by the following equation [23]:

$$a_{\text{retained austenite}} = 0.35467 + 0.00467 \text{ wt\% C} \quad (7)$$

Figs. 3b, c compares the trend of retained austenite variations as a function of tempering temperature after single, double or triple tempering. In both NiCrSi and NiCrMoV steels, a significant amount of retained austenite was observed after single tempering up to 400 °C. Additionally, the results suggested that a double or triple tempering did not considerably reduce the amount of retained austenite. It is clear that the retained austenite was stable up to 400 °C in both studied steels, regardless of the number of tempering stage. Of particular note was that the retained austenite was dramatically decomposed at the tempering temperature of

500 °C in both steels. This range of temperature is higher than reported temperatures for other grades of steel in the literature, suggesting a higher thermal resistant in the studied steels [8,

1 0] . T h e

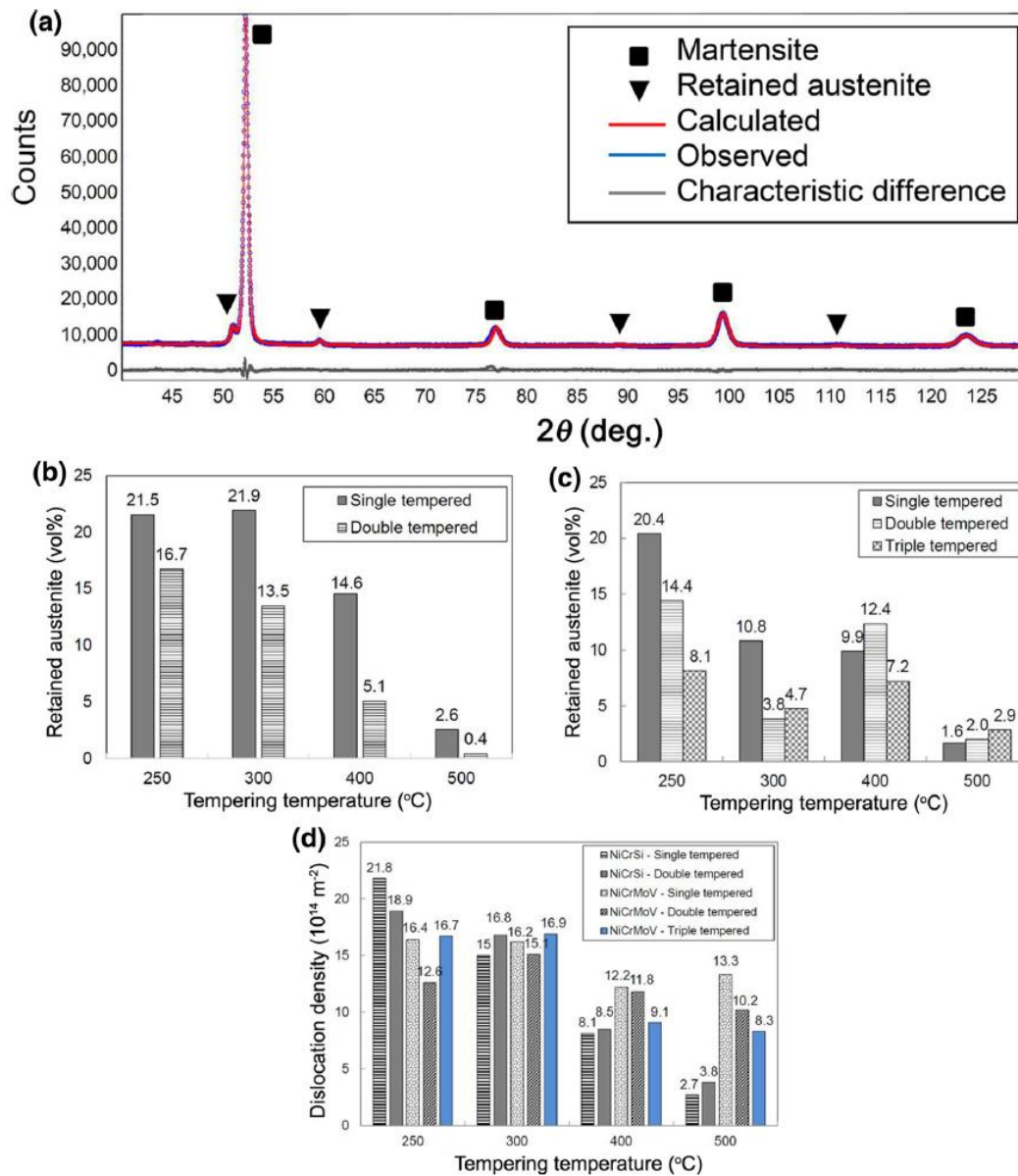


Fig. 3 Retained austenite volume fraction versus tempering temperature: (a) Selected XRD curves; (b) NiCrSi; (c) NiCrMoV (d) dislocation density measured according to WH method.

results showed that the retained austenite decomposition is rather sluggish and strongly dependent on the tempering temperature. Also, below a certain temperature range a double or triple tempering did not cause any significant retained austenite decomposition.

In both steels, the results showed a high level of carbon content in retained austenite after tempering up to 250 to 300 °C and dramatic reduction at higher tempering temperatures. The

results also suggested that double or triple tempering at 250 and 300 °C progressively increased the carbon content of retained austenite.

Table 2, The retained austenite characteristics determined from XRD results.

	T _{tempering} (°C)	NiCrSi		NiCrMoV		
		Single tempered	Double tempered	Single tempered	Double tempered	Triple tempered
Retained austenite (vol%)	250	21.5	16.7	20.4	14.4	8.1
	300	21.9	13.4	10.8	3.8	4.7
	400	14.5	5.0	9.8	12.3	7.2
	500	2.5	0.4	1.6	2.0	2.8
Carbon content (%)	250	1.20	1.24	1.16	1.17	1.18
	300	1.37	1.50	1.15	1.20	1.22
	400	1.04	1.17	1.09	1.03	1.10
	500	0.94	0.96	1.05	0.98	0.98
Lattice parameter (nm)	250	0.36032±0.00013	0.36048±0.00011	0.36009 ±0.00020	0.36017 ±0.00014	0.36021 ±0.00019
	300	0.36109±0.00011	0.36170±0.00017	0.36004±0.00017	0.36030±0.00017	0.36039±0.00021
	400	0.35953±0.00008	0.36016±0.00012	0.35979±0.00012	0.35949±0.00012	0.35983±0.00011
	500	0.35907±0.00009	0.35919±0.00018	0.35958±0.00014	0.35926±0.00013	0.35925±0.00011

Fig. 3d compares the variation of dislocation density of tempered samples. These results are comparable to other reports in the literature about the dislocation density of tempered martensitic steels, e.g. [24]. In NiCrSi steel, a progressive and considerable reduction in dislocation density was observed due to tempering temperature increases. However, double tempering did not significantly alter the dislocation density of NiCrSi steel. Generally, the results showed insignificant variations in the dislocation density of NiCrMoV steel after tempering at different temperatures and also after double or triple tempering, while triple tempering at 400 and 500 °C seems to slightly reduce the dislocation density. Moreover, random retesting confirmed that the variations in the amount of retained austenite in both steels were in the range of 1–4 wt%, while insignificant variations were observed in the average carbon content and dislocation density.

3.3. Hardness

Figs. 4 a and b show the hardness variation of NiCrSi and NiCrMoV steels after single, double or triple tempering at different temperatures, respectively. The results indicated no

significant difference in the hardness of samples after double or triple tempering in both steels. Clearly, the hardness variation after tempering is mainly associated with tempering temperature.

Fig. 4 c compares the trend of hardness variation as a function of tempering temperature for NiCrSi and NiCrMoV steels. Note that the presented data are focused on the single tempering, as the double and triple tempering did not show any hardness changes (Figs. 4 a and b). Interestingly, the results demonstrated different softening resistant in the studied steels with ascending order NiCrMoV steel > NiCrSi steel, particularly at temperatures over 300 °C. This is important, as it can significantly influence the wear behaviour of material, especially when frictional temperature rises can accelerate subsurface softening and enhance delamination wear [1].

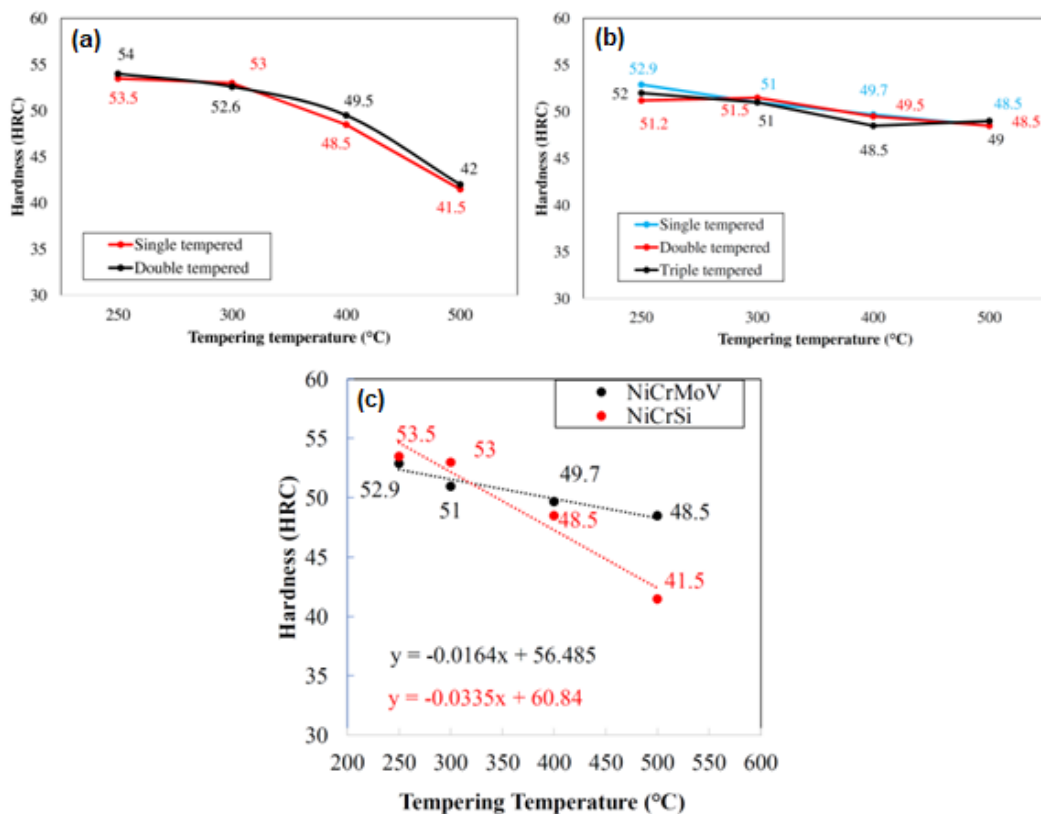


Fig. 4 Average hardness variations in terms of tempering temperature, (a) Single and double tempered NiCrSi steel, (b) Single, double and triple tempered NiCrMoV steel, (c) Comparison between single tempered NiCrSi and NiCrMoV steels.

3.4. Tensile Properties

Figs. 5 a and b indicate selected engineering stress-strain curves corresponding to double tempered NiCrSi steel and triple tempered NiCrMoV steel. Further details of tensile properties are shown in Table 3. In NiCrSi steel, the results evidenced a progressive softening

due to tempering temperature increases. Clearly, the strengths (i.e. flow stress and UTS) were reduced at the expense of ductility increases. In NiCrMoV steel, the results showed a similar flow stress (i.e. 0.2% offset proof stress) in tempered samples up to 300 °C, while tempering

a

t

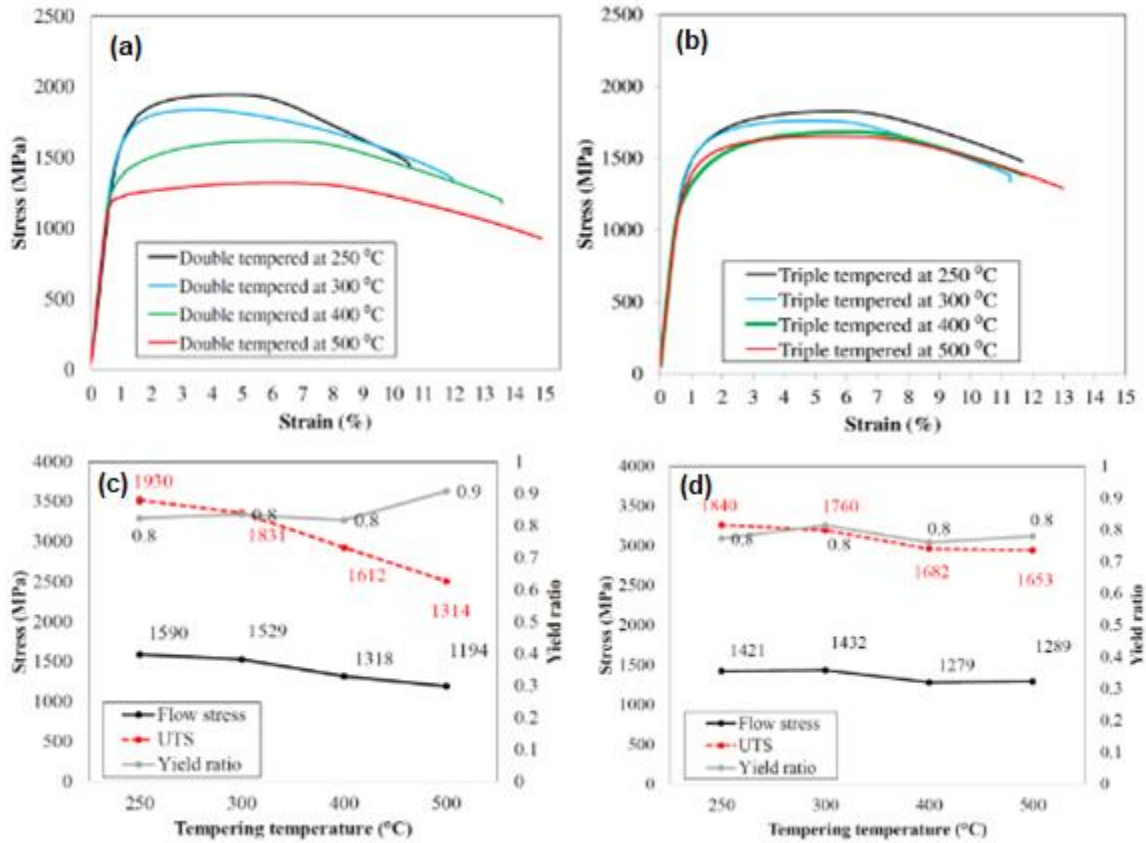


Fig. 5 (a) and (b) Engineering stress-strain curves of NiCrSi and NiCrMoV steels, respectively, (c) and (d) Trend of flow stress, UTS and yield ratio variations in NiCrSi and NiCrMoV steels, respectively.

temperatures ≥ 400 °C slightly reduced the flow stress. To assist interpretation of results, the yield ratio (flow-stress/UTS) was also calculated from tensile results (Figs. 4 (c) and (d)). The trend of yield-ratio shows a similar level after tempering at all temperatures in both steels. The results suggest that the work hardening up to UTS was not considerably changed due to tempering at different temperatures in both steels.

Table 3, A comparison between the tensile properties.

Steel	Tempered at 250 °C			Tempered at 300 °C			Tempered at 400 °C			Tempered at 500 °C		
	Yield strength	UTS (MPa)	e1%									

	(MPa)		(MPa)		(MPa)		(MPa)		(MPa)		(MPa)	
NiCrSi	1590±6	1930±11	9.5±0.5	1529±26	1831±5	10.5±0.5	1318±2	1612±5	12±1	1194±3	1314±7	13±2
NiCrMoV	1421±25	1840±11	9.6±1.1	1432±2	1760±5	9.6±1.1	1279±12	1682±1	10±1.7	1289±10	1653±1	12±1

3.5. Charpy Impact Toughness

Figure 6 shows the variation of average Charpy impact toughness in terms of tempering temperature in single- and double-tempered NiCrSi steel and in single- and triple-tempered NiCrMoV steel. The results showed a trough in the toughness plot of NiCrSi steel. By increasing the tempering temperature up to 400 °C, the results indicated a sudden toughness decrease from ~25 to ~14 J in both single- and double-tempered NiCrSi samples. However, tempering at 500 °C again slightly raised the toughness to ~16 J. This trend is consistent with other reports in the literature about tempered martensite embrittlement (TME) behaviour for medium-carbon steels, suggesting a TME at 400 °C [11, 25, 26]. The results also demonstrated that the toughness was not significantly changed in both single- and triple-tempered NiCrMoV samples due to tempering at different temperatures. It can be suggested that toughness variations in both steels were mainly dependent upon the first tempering stage and double/triple tempering did not influence the results.

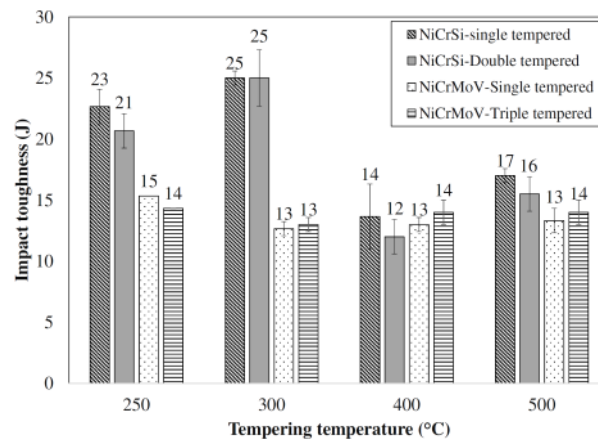


Fig. 6 Average Charpy impact toughness.

3.6. Fractography of Fractured Specimens

Figure 7 shows typical SEM micrographs corresponding to the tensile fracture surface of double-tempered NiCrSi and triple-tempered NiCrMoV steel samples. Tensile fracture surface in all samples appeared to be a cup-cone fracture surface. A dominant ductile dimple

fracture was observed in all samples, regardless of the tempering conditions. Interestingly, NiCrSi samples showed a Rosette fracture surface after tempering at 500 °C (Fig. 7g) [27]. Figure 8 indicates SEM micrographs corresponding to the Charpy specimen fracture surface of single-tempered NiCrSi steel and single-tempered NiCrMoV steel. As with the tensile specimens, a dominant dimple fracture appeared in all samples. From the SEM observations,

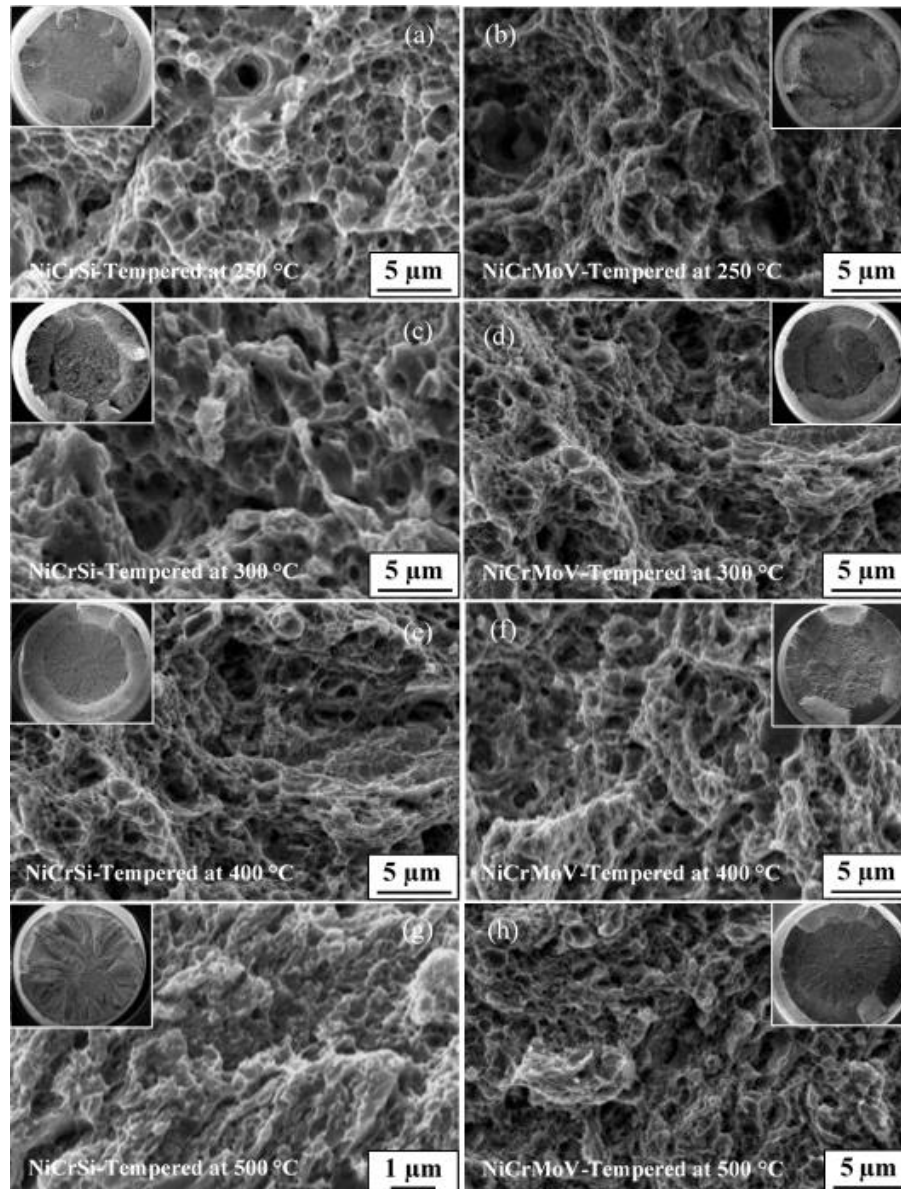


Fig. 7 SEM micrographs of tensile fracture surface of NiCrSi and NiCrMoV steels.

it was also found that the fracture surface was quite similar in single and double-tempered NiCrSi samples so that double tempering did not affect the fracture mode. However, by increasing the tempering temperature, especially C 400 °C, a higher frequency of quasi-cleavage features with a considerably larger facet size was observed in both single- and double-tempered NiCrSi samples. This shows good agreement with the observed impact

strength results and indicates that the TME (at 400 °C) mainly enhanced a quasi-cleavage fracture behaviour in NiCrSi samples. In NiCrMoV steel, quasi-cleavage fracture features were hardly observed and the dimple size was relatively finer than NiCrSi samples. However, the results showed insignificant difference in the fracture mode of NiCrMoV samples in terms of tempering temperature and after triple tempering. Additionally, no brittle intergranular fracture was observed in both steels, which is generally known as a sign of grain boundary weakening due to the segregation of alloying elements and impurities [26, 28].

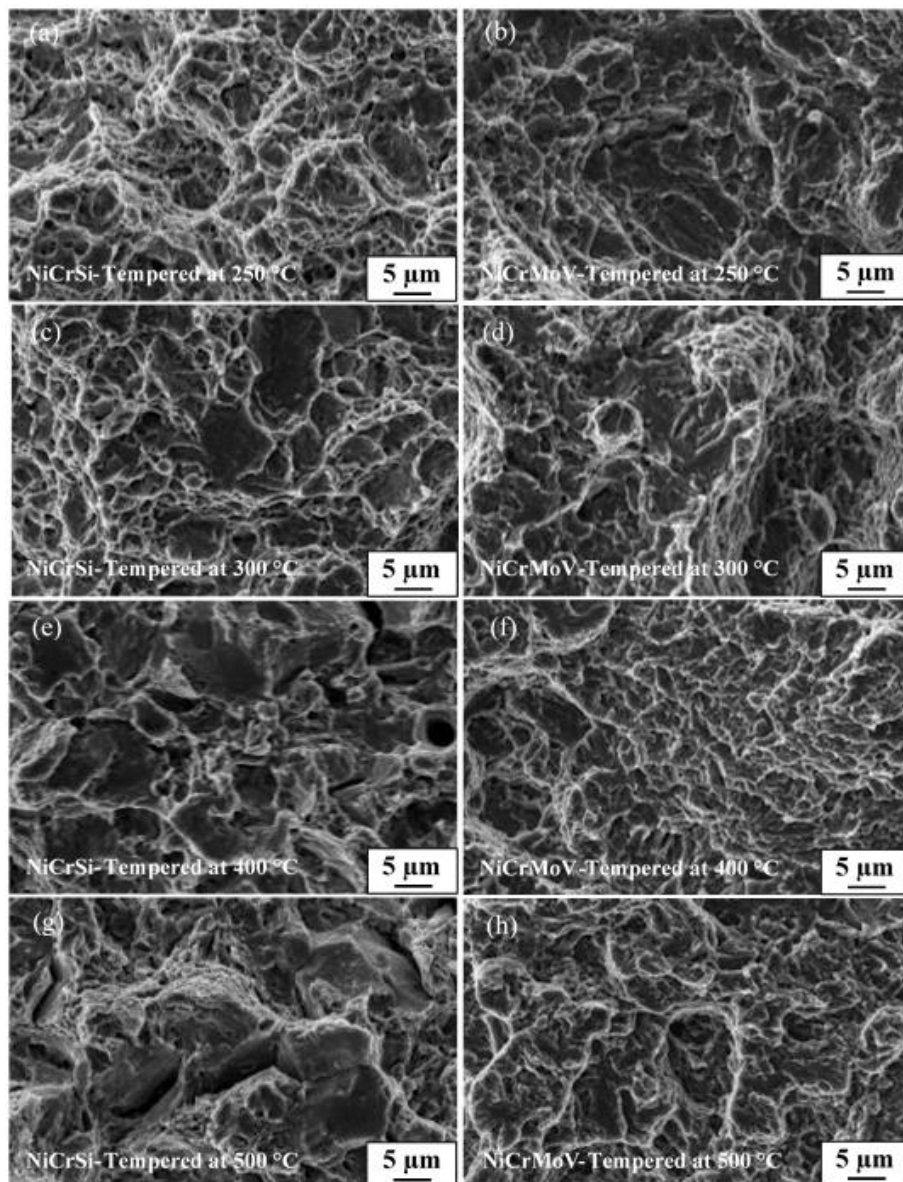


Fig. 8 SEM micrographs of Charpy impact fracture surface of NiCrSi and NiCrMoV steels.

4. Discussion

4.1. Microstructure

The microstructural evolution of the studied steels showed different behaviours at different tempering temperatures (Figs. 1, 2). In NiCrSi, the frequency of carbides was significantly and progressively raised with increasing tempering temperature, especially at boundaries after tempering at C 400 °C. This behaviour was ascribed to its chemical composition, in particular the effect of Si, Cr, Mo, Ni and Mn [7, 9, 28–30]. The solute carbon diffuses out from carbon-supersaturated martensite through high diffusion paths (e.g. boundaries) and can precipitate at early and prolonged stages of tempering [31]. However, the presence of the above-mentioned elements can differently control the precipitation behaviour of transition carbides and cementite at different tempering temperatures and holding times [6, 9, 32]. The chemical composition of NiCrSi steel is similar to AISI 4340 steel, but with higher amounts of Si and Ni [12, 26]. It has been well understood that these elements, especially Si, inhibit the dissolution of transition carbides and the formation and growth coarsening of cementite and also enhance the dissolution of cementite during tempering. In fact, a segregation of silicon around cementite nucleus can considerably and locally increase the activity of carbon, which prevents the flux of carbon to cementite nucleus [7, 33, 34]. The large density of precipitates in NiCrSi steel, in particular coarser interlath precipitates at C 400 °C, was attributed to cementite. As mentioned earlier, the bright filmy-shaped features were also reduced at the expense of formation of precipitates in NiCrSi steel. Presumably, the retained austenite was considerably decomposed and cementite was formed at C 400 °C in NiCrSi steel (Fig. 3). Similarly, the XRD results also showed a significant decomposition of retained austenite at this range of temperature in NiCrSi steel (Fig. 3). This is consistent with the results of other researchers who also reported a similar range of temperature for precipitation in other grades of steel, for example 300 M steels [14, 26].

In NiCrMoV steel, a high density of interlath and intralath precipitates were observed after tempering at 250 °C, while no considerable difference was seen at higher tempering temperatures up to 400 °C (Figs. 1, 2). Although it was outside the scope of this work to determine the nature of these precipitates, it is thought that they were mainly cementite and V-carbides. A higher level of carbon in NiCrMoV steel and lower Si content were likely the reasons for the accelerated precipitation from a lower tempering temperature, i.e. 250 °C. Moreover, tempering at 500 °C evidenced a slight spheroidisation of precipitates in both steels. Similarly, other researchers have reported a similar range of temperature for the spheroidisation of cementite in steels [6,21]. However, the microscopy observations showed no precipitate coarsening (Oswald-ripening) in NiCrMoV steel. It should be noted that the chemical composition of NiCrMoV steel is quite comparable to 300M steel, while its Si

content is as low as AISI 4340 steel and the levels of Ni and Cr are almost twice of 300M steel [12,26,35]. Ni and Cr not only can increase the toughness and strength of steels, especially during cryogenic treatments, but also they can retard the growth coarsening of precipitates during tempering [36-37]. Hence, a higher level of Ni and Cr might be the reason for insignificant growth-coarsening of precipitates in NiCrMoV steel, while 0.22 wt% Si failed to retard the precipitation at lower tempering temperatures.

SEM results also showed a very low frequency of relatively coarse martensite in NiCrSi steel, whereas this behaviour was hardly observed in NiCrMoV steel (Figs. 1,2). It is thought that the observed difference in the morphology of martensite was mainly attributed to the effect of V and Mo additions and a higher level of C, Ni and Cr, which might further enhance the refinement of martensite in NiCrMoV steel during identical quenching conditions [20]. Moreover, it was found that the lath shaped tempered-martensite was reluctant to any growth-coarsening during the applied tempering processes. The straight sides of lath shaped martensite are low-energy and coherent/semi-coherent boundaries and therefore immobile [10,39]. These structures require a higher level of energy for lateral growth/coarsening. It is thus clear that the tempering processes did not change the size and morphology of lath tempered martensite in both steels.

4.2. Retained Austenite

The XRD results of NiCrSi steel showed a decrease in the amount of retained austenite after tempering at 400 °C (Fig. 3 and Table 2). In NiCrMoV steel, the retained austenite gradually reduced by increasing the tempering temperature, though a significant amount of retained austenite was still remained in the microstructure below 500 °C.

The XRD results also showed that the carbon content of retained austenite was raised after double or triple tempering at 250-300 °C in both steels, while higher tempering temperatures reduced its carbon level (Table 2). As the samples were quenched in oil down to about 100 °C, a partitioning of carbon from martensite to retained austenite during subsequent tempering might increase its carbon content. This is similar to conventional quenching-partitioning processes, though our initial quenching temperature (i.e. 100 °C) was significantly lower than other reported temperatures in the literature [40]. Moreover, it has been shown that transition carbides are thermally unstable at higher tempering temperatures (e.g. ~300 °C) and they can be dissolved in the microstructure [41]. Perhaps, the presence of carbon solute and slow kinetics of Fe₃C precipitation due to the presence of Si could enhance the partitioning of carbon into retained austenite. Nevertheless, a gradual precipitation at

higher temperatures in both steels could reduce the carbon content of retained austenite and consequently enhance the decomposition of retained austenite (Table 2) [26]. Additionally, the slight fluctuation in the carbon content of retained austenite, especially at higher tempering temperatures, might be related to the morphology of retained austenite and precipitation during tempering.

Double or triple tempering of both NiCrSi and NiCrMoV steels showed a very slight reduction in the amount of retained austenite (Fig. 3). It is generally desirable to completely decompose the un/meta-stable retained austenite (with $C_c \approx 1\%$) during tempering to avoid the formation of fresh martensite from retained austenite, especially under impact or fatigue loading conditions [3, 42]. This may endanger the performance of components and cause rapid fracture. However, our results confirmed the earlier conclusions about the microstructural variations, suggesting that the retained austenite decomposition was strongly dependent on temperature rather than the number of tempering stages in the studied steels.

4.3. Mechanical Properties

The present paper reports on the tensile properties of double tempered NiCrSi steel, and triple tempered NiCrMoV steel. Moreover, the Charpy impact results correspond to the single and double tempered NiCrSi steel and the single and triple tempered NiCrMoV steel.

4.3.1 Hardness and Flow Stress

A comparison between the hardness values of single-, double- or triple-tempered samples showed that the hardness variation is mainly controlled by the tempering temperature in both steels (Fig. 4). In fact, double or triple tempering did not significantly change the hardness of the studied steels. Similarly, the tensile results suggested a progressive softening due to tempering temperature increases in NiCrSi steel, while no considerable softening was observed in NiCrMoV steel (Fig. 4c). According to the SEM and XRD analysis, the strength/hardness variations were mainly attributed to the carbon content and dislocation density of martensite, precipitate strengthening and retained austenite volume fraction. In fact, the diffusion of carbon from carbon-supersaturated martensite to high diffusion paths, especially boundaries, and reduction of dislocation density and the presence of retained austenite would have resulted in softening of steel.

In NiCrSi steel, a progressive dislocation density reduction was observed with increasing tempering temperature (Fig. 3c). Furthermore, the presence of precipitates in the

microstructure evidenced a possible reduction of carbon from carbon-supersaturated martensite. It is well known that the retained austenite is softer than martensite and a larger fraction of retained austenite can enhance the softening. In this context, the results showed no meaningful relationship between the volume fraction of retained austenite and softening in the studied steels. Furthermore, a gradual decomposition of retained austenite to ferrite could also further enhance the softening, though the newly formed carbides might contribute to strengthening of steel. However, the results showed that the softening effect of the above-mentioned mechanisms was more pronounced than the possible hardening effect of carbide precipitates. This is consistent with the results of other researchers who also reported a similar behaviour for tempered steels [28]. It can be thus inferred that the main reason for the softening of NiCrSi steel was mainly attributed to the dislocation annihilation/rearrangement and reduction of solute carbon from carbon-supersaturated martensite.

As noted earlier, the results showed a marginal hardness reduction in NiCrMoV steel after tempering (Fig. 4). In this way, the XRD analysis did not show a considerable variation in the dislocation density of NiCrMoV steel after tempering (Fig. 3). The SEM observations also showed insignificant variations in the size and density of precipitates during tempering and after double and triple tempering (Figs. 1, 2). Although there are no available data about the nature of precipitates in the present paper, it is thought that the observed precipitates are associated with cementite and V-carbide. It has been shown in the literature that Fe₃C carbides are not very effective in retarding the recovery of martensite during tempering, though transition carbides can inhibit the softening at early stages of tempering [32, 43]. Additionally, recent studies on the effect of V-carbide precipitates have shown that these precipitates can strongly retard the recovery of microstructure during prolonged tempering [23, 28, 43]. It can be thus suggested that the presence of V-carbides might be the main reason for the higher softening resistance of NiCrMoV steel. The results also showed a slight hardness/strength reduction after tempering at 500 °C in both steels (Figs. 4, 5). This was mainly ascribed to the further recovery and carbon content reduction of martensite and also the spheroidisation of carbides, as shown in Figs. 1g, h and 2g, h. Similarly, other researchers have shown in the literature that the spheroidisation of carbides during tempering can enhance the softening of steels [5, 6].

4.3.2. Impact Toughness

A significant difference was observed in the trend of impact toughness variations in the studied steels after tempering from 250 to 500 °C (Fig. 6). The toughness of NiCrSi steel was suddenly and remarkably reduced at 400 °C, followed by a slight increase after tempering at 500 °C. In contrast, the results evidenced a rather similar level of toughness after tempering at all tempering temperatures in NiCrMoV steel (Fig. 6).

As with the tensile specimens, a dominant dimple fracture appeared in all Charpy samples. From the SEM observations, it was also found that the fracture surface was quite similar in single- and double-tempered NiCrSi samples, and double tempering did not affect the fracture mode. By increasing the tempering temperature, especially C 400 °C, a higher frequency of quasi-cleavage features with a considerably larger facet size was observed in both single- and double-tempered NiCrSi steel (Fig. 8e, g). This behaviour is similar to a classic tempered martensite embrittlement in steels [13, 26]. It has been established that the TME is mainly related to interlath carbide precipitates and also mechanically unstable retained austenite [5, 13, 41]. In this case, our SEM and XRD observations evidenced a significant precipitation and reduction in the volume fraction of retained austenite after tempering at temperatures of C 400 °C (Figs. 1, 2 and Table 2). The lower carbon content of retained austenite would have reduced the mechanical stability of retained austenite which might contribute to the decrease of the impact toughness of NiCrSi steel [42, 44]. It can be thus inferred that the observed phenomenon at 400 °C is primarily related to tempered martensite embrittlement, resulting from the carbide precipitation and unstable retained austenite. However, further softening of material due to tempering at 500 °C slightly neutralised the embrittlement (Fig. 4) [26].

In NiCrMoV steel, the impact toughness results evidenced a rather constant value at all tempering temperatures, regardless of variations in the dislocation density and retained austenite volume fraction (Figs. 3, 6). The results suggested that the toughness of NiCrMoV steel was less likely influenced by the retained austenite and dislocation density. In this way, the fractography of fracture samples also showed dominant ductile fracture with fine dimple features in all samples. However, a significant density of inter-/intra-lath precipitates was observed in the microstructure of NiCrMoV steel after tempering at 250 °C, while it was not considerably changed at higher tempering temperatures. The results suggested that the toughness behaviour of NiCrMoV steel might be mainly affected by the precipitation behaviour. This will be further clarified next.

The SEM results suggested insignificant difference in the size of martensite after tempering at different temperatures in both steels (Fig. 1). Moreover, previous studies have shown similar average prior austenite grain size and non-metallic inclusions size in NiCrSi and NiCrMoV steels, though the density of inclusions was qualitatively higher in the former steel [20]. Our toughness results ruled out the effect of inclusions and prior austenite grain size on the observed difference in the toughness of the studied steels after tempering (Fig. 6). However, the toughness of NiCrSi steel was reduced after tempering at 400 °C to the same level as that observed in NiCrMoV steel (Fig. 6). Considering a similar size and morphology of martensite after tempering at different temperatures, the presence of large precipitates in NiCrSi steel after tempering at 400 °C and in NiCrMoV steel could promote easier crack path and reduce the impact toughness [35, 44]. Similarly, other researchers have reported that the formation of carbides during tempering can reduce the toughness of steels [41, 45]. Moreover, a slightly higher level of carbon in NiCrMoV steel might be another reason for its lower impact toughness compared to NiCrSi steel. It can be suggested that the main reason for the relatively lower toughness of NiCrMoV steel compared to NiCrSi steel was primarily related to the effect of precipitates and carbon content.

4.3.3. Total Elongation

The tensile results showed a progressive increase in the total elongation of both steels by increasing tempering temperature (Fig. 5a, b and Table 3). It was also found that the total elongations of NiCrSi steel were slightly higher than NiCrMoV steel. This was mainly attributed to the softening mechanisms during tempering process, i.e. lower carbon content and dislocation annihilation of tempered martensite. The fracture surface of both steels also showed dominant dimple features in all samples, indicating a ductile fracture mode in both steels (Fig. 7). Interestingly, the fracture surface of NiCrSi steel after tempering at 500 °C showed a Rosette fracture feature (Fig. 7g). However, the remaining samples exhibited an ordinary cup-and-cone fracture surface. It is well known that precipitation at martensite lath boundaries can mainly cause Rosette fracture surface [27, 46]. This agrees with earlier conclusions about the microstructure of quenched-tempered samples, suggesting that the carbide precipitation at boundaries was mainly responsible for this behaviour in NiCrSi steel (Figs. 1g, 2g).

5. Conclusions

- 1- The hardness results suggested that hardness reduction after tempering is primarily controlled by tempering temperature. However, double and triple tempering at the same temperature did not considerably change the hardness of both steels.
- 2- Tensile flow stress and hardness results showed that NiCrMoV steel showed a higher temper resistant compared to NiCrSi steel, especially at temperatures over 300 °C. This was mainly ascribed to the effect of V-addition.
- 3- The XRD analysis indicated that retained austenite decomposition is mainly dependent upon the tempering temperature. It was also found that double or triple tempering at the same temperature did not considerably reduce the retained austenite.
- 4- The toughness of NiCrMoV steel was rather similar after tempering at different temperatures, while NiCrSi steel showed a sudden toughness reduction after tempering at 400 °C. The observed difference was ascribed to the precipitation behaviour during tempering at different temperatures.

Acknowledgment

The authors would like to acknowledge the sponsorship provided by Innovate UK through the Knowledge Transfer Partnership programme (KTP010269 Sheffield Hallam University & Tyzack Machine Knives Ltd.).

References

- [1] E.Abbasi, Q.Luo and D.Owens, "Case Study: Wear Mechanisms of NiCrVMo-steel and CrB-steel Scrap Shear Blades," *Wear*, vol. 398–399, p. 29–40, 2018.
- [2] Y.Wang, T.Lei and J.Liu, "Tribo-metallographic Behavior of High Carbon Steels in Dry Sliding II. Microstructure and Wear," *Wear*, vol. 231, pp. 12-19, 1999.
- [3] Y.Tomita, "Development of Fracture Toughness of Ultrahigh Strength, Medium Carbon, Low Alloy Steels for Aerospace Applications," *International Materials Reviews*, vol. 45, no. 1, pp. 23-27, 2000.
- [4] M.Assefpour-Dezfuly and A.Brownrigg, "Parameters Affecting Sag Resistance in Spring Steels," *Metallurgical Transactions A*, vol. 20, no. 10, pp. 1951-1959, 1989.
- [5] G.Krauss, "Tempering of Lath Martensite in Low and Medium Carbon Steels: Assessment and Challenges," *Steel Research International*, vol. 77, no. 10, pp. 1-18, 2017.
- [6] W.J.Nam, C.S.Lee and D.Y.Ban, "Effects of Alloy Additions and Tempering Temperature on the Sag Resistance of Si-Cr Spring Steels," *Materials Science and Engineering A*, vol. 289, pp. 8-17, 2000.

- [7] G.R.Speich and W.C.Leslie, "Tempering of Steel," *Metallurgical Transactions*, vol. 3, no. 5, pp. 1043-1054, 1972.
- [8] M.Jung, S.J.Lee and Y.K.Lee, "Microstructural and Dilatational Changes during Tempering and Tempering Kinetics in Martensitic Medium Carbon Steel," *Metallurgical and Materials Transactions A*, vol. 40, no. 3, p. 551–559, 2009.
- [9] F.Nazemi, J.Hamel-Akré and P.Bocher, "Modeling of Cementite Coarsening during Tempering of Low-alloyed-medium Carbon Steel," *Journal of Materials Science*, vol. 53, pp. 6198-6218, 2018.
- [10] D.A.Porter, K.E.Easterling and M.Sherif, *Phase Transformations in Metals and Alloys*, Third ed., CRC Press , 2009.
- [11] L.C.F.Canale, R.A.Mesquita and G.E.Totten, *Failure Analysis of Heat Treated Steel Components*, Ohio : ASM International, 2008.
- [12] W.M.Garrison, "High Toughness Secondary Hardening Steels with Nickel as a Primary Strength and Toughening Agent". Patent US2016/0237535 A1, 18 August 2016.
- [13] H.K.D.H.Bhadেশia, "Prevention of Hydrogen Embrittlement in Steels," *ISIJ International*, vol. 56, no. 1, p. 24–36, 2016.
- [14] A.J.Clark, M.K.Miller, R.D.Field, D.R.Coughlin, P.J.Gibbs, K.D.Clark, D.J.Alexander, K.A.Powers, P.A.Papin and G.Krauss, "Atomic and Nanoscale Chemical and Structural Changes in Quenched and Tempered 4340 Steel," *Acta Materialia*, vol. 77, pp. 17-27, 2014.
- [15] A.K. Sinha, B.P. Division, *Defects and Distortion in Heat Treated Parts* (ASM International, Russell, 1991)
- [16] X.Luo and G.E.Totten, "Analysis and Prevention of Quenching Failures and Proper Selection of Quenching Media: An Overview," *Journal o ASTM International* , vol. 8, no. 4, pp. 1-29, 2011.
- [17] A.K.Sinha and B.P.Division, "Defects and Distortion in Heat Treated Parts," in *ASM Handbook : Heat Treating*, vol. 4, ASM International, 1991, pp. 601-619.
- [18] A.K.Sinha and B.P.Division, "Defects and Distortion in Heat-Treated Parts," in *ASM Handbook, Volume 4: Heat Treating*, vol. 4, ASM International, 1991, pp. 601-619.
- [19] E. Abbasi, *Wear Behaviour of CBS, HISI and W1.2746 Steels* (Sheffield Hallam University, Sheffield, 2017)
- [20] E. Abbasi, Q. Luo, D. Owens, A comparison of microstructure and mechanical properties of low-alloy-medium-carbon steels after quench-hardening, *Mater. Sci. Eng. A* 725, 65 (2018)
- [21] C.L.Briant, "Role of Carbides in Tempered Martensite Embrittlement," *Materials Science and Technology*, vol. 5, no. 2, pp. 138-147, 1989.
- [22] W.S.Lee and T.T.Su, "Mechanical Properties and Microstructural Features of AISI 4340 High-

- strength Alloy Steel under Quenched and Tempered Conditions," *Journal of Materials Processing Technology*, vol. 87, pp. 198-206, 1999.
- [23] E.Abbasi and W.M.Rainforth, "Microstructural Evolution during Bainite Transformation in a Vanadium Microalloyed TRIP-assisted Steel," *Materials Science & Engineering A*, vol. 651, pp. 822-830, 2016.
- [24] B.Kim, E.Boucard, T.Sourmail, D.S.Martín, N.Gey and P.E.J.Rivera-Díaz-del-Castillo, "The Influence of Silicon in Tempered Martensite: Understanding the Microstructure–Properties Relationship in 0.5–0.6 wt.% C Steels," *Acta Materialia*, vol. 68, pp. 169-178, 2014.
- [25] Ph.Lemle, A.Pineau, J.L.Castagne and Ph.Dumoulin, "Temper Embrittlement in 12%Cr Martensitic Steel," *Metal Science*, vol. 13, no. 8, pp. 496-502, 1979.
- [26] R.M.Horn and R.O.Ritchie, "Mechanisms of Tempered Martensite Embrittlement in Low Alloy Steels," *Metallurgical Transactions A*, vol. 9, no. 8, pp. 1039-1053, 1978.
- [27] P.Verma, G.S.Rao, N.C.S.Srinivas and V.Singh, "Rosette Fracture of Modified 9Cr-1Mo Steel in Tension," *Materials Science and Engineering A*, vol. 683, pp. 172-186, 2017.
- [28] L.Å.Norström, "The Relation Between Microstructure and Yield Strength in Tempered Low-carbon Lath Martensite with 5% Nickel," *Metal Science*, vol. 10, no. 12, pp. 429-436, 1976.
- [29] J.Liu, H.Yu, J.Wang, T.Zhou and C.Song, "Effect of Tempering Temperature on Microstructure Evolution and Mechanical Properties of 5% Cr Steel via Electro-Slag Casting," *Steel Research International*, vol. 86, no. 9, pp. 1082-1089, 2015.
- [30] W.J.Nam and C.S.Lee, "Microstructural Influence on Sag Resistance of Cr Containing and Cr Free Spring Steels," *Materials Science and Technology*, vol. 14, no. 8, pp. 827-831, 1998.
- [31] S.Sackl, M.Zuber, H.Clemens and S.Primig, "Induction Tempering vs Conventional Tempering of a Heat-Treated Steel," *Metallurgical and Materials Transactions A*, vol. 47, no. 7, pp. 3694-3702, 2016.
- [32] Y.Xiao, W.Li, H.S.Zhao, X.W.Lu and X.J.Jin, "Investigation of Carbon Segregation during Low Temperature Tempering in a Medium Carbon Steel," *Materials Characterization*, vol. 117, pp. 84-90, 2016.
- [33] A.Zhang, G.Wang and S.Jia, "Ultrahigh-Strength Wear-Resistant Steel Plate and Method of Manufacturing the Same". Patent US 2014/0124102 A1, 8 May 2014.
- [34] T.Sakuma, N.Watanabe and T.Nishizawa, "The Effect of Alloying Element on the Coarsening Behavior of Cementite Particles in Ferrite," *Transactions of the Japan*, vol. 21, no. 3, pp. 159-168, 1980.
- [35] Y.Tomita and T.Okawa, "Effect of Microstructure on Mechanical Properties of Isothermally Bainite-transformed 300M Steel," *Materials Science and Engineering A*, vol. 172, pp. 145-151,

1993.

- [36] J.Krawczyk, P.Bala and J.Pacyna, "The Effect of Carbide Precipitate Morphology on Fracture Toughness in Low Tempered Steels Containing Ni," *Journal of Microscopy*, vol. 237, no. 3, pp. 411-415, 2010.
- [37] Y.Tomita and K.Okabayashi, "Heat Treatment for Improvement in Lower Temperature Mechanical Properties of 0.40 Pct C-Cr-Mo Ultrahigh Strength Steel," *Metallurgical Transactions A*, vol. 14, no. 11, pp. 2387-2393, 1983.
- [38] M.Niikura and J.W.Morris, "Thermal Processing of Ferritic 5Mn Steel for Toughness at Cryogenic Temperatures," *Metallurgical Transactions A*, vol. 11, no. 9, p. 1531–1540, 1980.
- [39] E.Abbasi and W.M.Rainforth, "Effect of Nb-Mo Additions on Precipitation Behaviour in V Microalloyed TRIP-assisted Steels," *Materials Science and Technology*, vol. 32, no. 16, pp. 1721-1729, 2016.
- [40] J.G.Speer, E.D.Moor, K.O.Findley, D.K.Matlock, B.C.D.Cooman and D.V.Edmonds, "Analysis of Microstructure Evolution in Quenching and Partitioning Automotive Sheet Steel," *Metallurgical and Materials Transactions A*, vol. 42, pp. 3591-3601, 2011.
- [41] H.Bhadeshia and D.V.Edmonds, "Tempered Martensite Embrittlement: Role of Retained Austenite and Cementite," *Metal Science*, vol. 13, no. 6, pp. 325-334, 1979.
- [42] R. Wu, W. Li, S. Zhou, Y. Zhong, L. Wang, X. Jin, Effect of Retained Austenite on the Fracture Toughness of Quenching and Partitioning (Q&P)-Treated Sheet Steels, *Metall. Mater. Trans. A* 45, 1892 (2014)
- [43] D.Delagnes, F.Pettinari-Sturmel, M.H.Mathon, R.Danoix, F.Danoix, C.Bellot, P.Lamesle and A.Grellier, "Cementite-free Martensitic Steels: A New Route to Develop High Strength/High Toughness Grades by Modifying the Conventional Precipitation Sequence during Tempering," *Acta Materialia*, vol. 60, pp. 5877-5888, 2012.
- [44] Y.Zou, Y.B.Xu, Z.P.Hu, X.L.Gu, F.Peng, X.D.Tan, S.Q.Chen, D.T.Han, R. Misra and G.D.Wang, "Austenite Stability and Its Effect on the Toughness of a High Strength Ultra-low Carbon Medium Manganese Steel Plate," *Materials Science&EngineeringA* , vol. 675, p. 153–163, 2016.
- [45] P.Michaud, D.Delagnes, P.Lamesle, M.H.Mathon and C.Levailant, "The Effect of the Addition of Alloying Elements on Carbide Precipitation and Mechanical Properties in 5% Chromium Martensitic Steels," *ACTA Materialia*, vol. 55, no. 14, pp. 4877-4889, 2007.
- [46] W.R.Clough, R.M.Vennett and R.J.Hrubec, "The Rosette Star, Tensile Fracture," *Journal of Basic Engineering*, vol. 90, no. 1, pp. 21-27, 1968.